University of Wollongong
Research Online

Faculty of Engineering - Papers (Archive)

Faculty of Engineering and Information Sciences

2008

SiC and Carbon Nanotube Distinctive Effects on the Superconducting Properties of Bulk MgB2

G. Serrano
Instituto Balseiro-Centro Atómico Bariloche, Argentina

A. Serquis
Instituto Balseiro-Centro Atómico Bariloche, Argentinag

S X. Dou
University of Wollongong, shi@uow.edu.au

Saeid Soltanian
University of Wollongong, saeid@uow.edu.au

L. Civale
Los Alamos National Laboratory, New Mexico

See next page for additional authors

Follow this and additional works at: https://ro.uow.edu.au/engpapers

 Part of the Engineering Commons

https://ro.uow.edu.au/engpapers/456

Recommended Citation

Serrano, G.; Serquis, A.; Dou, S X.; Soltanian, Saeid; Civale, L.; Maiorov, B.; Holesinger, T. G.; Balakirev, F.; and Jaime, M.: SiC and Carbon Nanotube Distinctive Effects on the Superconducting Properties of Bulk MgB2 2008.
https://ro.uow.edu.au/engpapers/456

Research Online is the open access institutional repository for the University of Wollongong. For further information contact the UOW Library: research-pubs@uow.edu.au

Authors

G. Serrano, A. Serquis, S X. Dou, Saeid Soltanian, L. Civale, B. Maiorov, T. G. Holesinger, F. Balakirev, and M. Jaime

This journal article is available at Research Online: https://ro.uow.edu.au/engpapers/456

SiC and carbon nanotube distinctive effects on the superconducting properties of bulk MgB_2

G. Serrano and A. Serquis[a)]
Instituto Balseiro-Centro Atómico Bariloche CONICET, S. C. De Bariloche, 8400 Rio Negro, Argentina

S. X. Dou and S. Soltanian
Institute for Superconducting and Electronic Materials, University of Wollongong, Northfields Ave., Wollongong, New South Wales 2522, Australia

L. Civale, B. Maiorov, and T. G. Holesinger
Superconductivity Technology Center, Los Alamos National Laboratory, MS K763, Los Alamos, New Mexico 87545, USA

F. Balakirev and M. Jaime
National High Magnetic Field Laboratory, Los Alamos National Laboratory, MS E536, Los Alamos, New Mexico 87545, USA

(Received 15 September 2007; accepted 23 November 2007; published online 22 January 2008)

This work describes in detail the simultaneous enhancement of the upper critical field (H_{c2}) and the critical current density (J_c) of MgB_2 bulk samples doped with nano-SiC particles, as well as single-walled and double-walled (dw) carbon nanotubes (CNTs). The magnetization properties were examined in a superconducting quantum interference device magnetometer, and four-probe transport measurements were performed using a 50 T pulsed magnet to determine $H_{c2}(T)$. We found that the J_c enhancement is similar in all doped samples at 5 K but nano-SiC addition is more effective to improve the flux pinning in the high temperature range ($T \geqslant 20$ K); this improvement cannot solely be attributed to the C incorporation to the lattice but also to the presence of other types of defects (i.e., several kinds of nanoinclusions). CNTs produce a better C incorporation that is more effective to enhance H_{c2} [i.e., dwCNT-doped samples reached a record $H_{c2}(0) \sim 44$ T value for bulk MgB_2]. All the H_{c2}(T) curves obtained for different types of doping can be successfully described using a model for a two-gap superconductor in the dirty limit. © *2008 American Institute of Physics*. [DOI: 10.1063/1.2832463]

I. INTRODUCTION

Technological applications of MgB_2 superconductor are directly linked to the enhancement of its critical current density (J_c) and the upper critical field (H_{c2}). The pinning force may be improved by the incorporation of defects (nanoparticle doping, chemical substitutions, etc.).[1–6] On the other hand, the doping level affects the interband scattering coefficients $\Gamma_{\sigma\pi}$, $\Gamma_{\pi\sigma}$ and the diffusivity of each band D_σ, D_π, as predicted by Gurevich *et al.*,[7–11] and these changes may cause a significant H_{c2} variation. Earlier attempts succeeded in raising the intragrain J_c through the incorporation of $Mg(B_{1-x}O_x)_2$,[1] SiC,[2,12,13] Al,[3] Dy_2O_3,[4] nano-C,[5] and carbon nanotubes,[6,12,14–16] which produce a decrease in the critical temperature (T_c) by chemical substitution and probably lattice strain.[17] The improvement of intergrain J_c in bulk samples is related to grain connectivity[18] and may be achieved by optimizing the processing parameters (i.e., ultrasonication,[16] HIPing,[18] applying magnetic field during the sintering process,[19] etc.). The best results for $H_{c2}(0)$ and J_c at high field ($H > 5$ T) and 4 K in polycrystalline samples were achieved using C and SiC, respectively. Although the effect of carbon substitution is one of the most studied in MgB_2, the results on C solubility and the effect of C doping on T_c, J_c, and H_{c2} reported so far vary significantly, due to precursor materials, fabrication techniques, and processing conditions used.[20–25] Recently, Matsumoto *et al.*[26] reported that J_c in SiC-alloyed MgB_2 tapes depends on a complex relation between grain connectivity, H_{c2}, and flux pinning induced by grain boundaries and precipitates. However, the distinct effect of C incorporation through different routes in J_c and H_{c2} is still not entirely understood.

The purpose of this work is to understand the role of C substitution and other defects on J_c and H_{c2} of bulk MgB_2 by studying samples doped with optimum content of SiC, single-walled (sw), and double-walled (dw) carbon nanotubes (CNTs). We found that all these additions simultaneously produce the enhancement of J_c and H_{c2}. The enhancement of J_c is similar at low temperatures in all three samples, but nano-SiC-doped sample has higher J_c at 20 K, indicating that the pinning is stronger in this sample due to the presence of other types of defects (i.e., Mg_2Si and other nonsuperconducting nanoinclusions). Record values of $H_{c2}(4\text{ K}) = 41.9$ T [with extrapolated $H_{c2}(0) \sim 44$ T] are reached for dwCNT addition that correspond to the highest C-substitution level achieved.

II. EXPERIMENTAL

Nano-SiC-doped samples were prepared using a reaction *in situ* technique.[12] Magnesium (−325 mesh, 99%) and amor-

[a)]Electronic mail: aserquis@cab.cnea.gov.ar.

 © 2008 American Institute of Physics

Downloaded 04 Sep 2008 to 130.130.37.13. Redistribution subject to AIP license or copyright; see http://jap.aip.org/jap/copyright.jsp

TABLE I. Nominal composition, synthesis temperature (T_s), lattice parameters, actual C content (x) calculated from a-axis values, and T_c as determined from the onset of the superconducting transition.

Sample	Nominal additions	T_s (°C)	a (Å)	c (Å)	x (at. %)	T_c (K)
Undoped	0%	900	3.0844(3)	3.526(1)	0	38.5 ± 0.5
SiC	nano-SiC 10 wt %	700	3.0770(5)	3.522(1)	0.022 (1)	37 ± 0.5
swCNT	swCNT 10 at. %	900	3.076(1)	3.524(1)	0.028 (2)	36 ± 0.5
dwCNT	dwCNT 10 at. %	900	3.0707(5)	3.527(1)	0.044 (1)	33.3 ± 0.5

phous boron (99%) were mixed with commercial 10 wt % SiC (20 nm). The mixed powders were uniaxialy pressed into pellets of 10 mm in diameter and 2 mm in thickness, sealed in an Fe tube and then heated at temperatures 700 °C for 1 h in flowing high purity Ar. This was followed by furnace cooling to room temperature. Undoped and CNT-doped MgB_2 samples were also prepared by solid-state reaction with 0 and 10 at. % nominal C contents, respectively, with similar starting materials, and single-walled (diameter of 1.1 nm, length of 0.5–100 μm, Aldrich) or double-walled carbon nanotubes (diameter of 1.3–5 nm, length of $\leqslant$50 μm, 90% Aldrich) as the source of carbon. The powders were grinded under nitrogen atmosphere inside a glovebox and pressed under ~500 MPa into small pellets with dimensions of 6 mm in diameter and ~4 mm in thickness, wrapped together with extra 20 at. % Mg turnings (99.98% Puratronic) in Ta foil and then placed in an alumina crucible inside a tube furnace in flowing Ar/H_2 at 900 °C for 30 min. The synthesis temperatures were the optimal ones for each kind of doping.[5,11]

In both cases (SiC and CNT) part of carbon dissolves into the MgB_2 structure during the fabrication process,[13,19] and the shift in the a-lattice parameter, obtained from x-ray diffraction, can be used as a measure of the actual amount of C (x) in the $Mg(B_{1-x}C_x)_2$ structure.[22] The synthesis temperature, lattice parameters, and x values obtained from fitting the single crystal data of Kazakov *et al.*[25] and the neutron diffraction data of Avdeev *et al.*[27] are listed in Table I.

III. RESULTS AND DISCUSSION

Figure 1 shows the normalized dc magnetization as a function of temperature (T), measured with a Quantum Design® superconducting quantum interference design magnetometer, in a field of 20 Oe using a zero field cooling process. The ΔT_c (90%–10%) of the superconducting transitions are lower than 1 K in all cases (except in sample with swCNT $\Delta T_c \sim 2$ K) indicating a homogeneous distribution of the C incorporated into the lattice. The inset displays the correlation between T_c and x for all samples listed in Table I. We observe the same dependence reported in previous works.[22,25,28]

The $H_{c2}(T)$ dependence was obtained from four-probe transport measurements in a 200 ms midpulse magnet up to 50 T at NHMFL-LANL, performed at temperatures between 1.4 and 35 K. Figure 2(a) displays the H_{c2} defined as the onset (extrapolation of maximum slope up to normal state resistivity) of the R versus H data as a function of the reduced temperature $t=T/T_{c0}$, where $T_{c0}=39$ K (Ref. 29) for all samples, as listed in Table II. The lines are fits to the data with the model proposed by Gurevich.[7] The fitting parameters in the model are the intraband electron diffusivities D_σ and D_π, and the interband scattering rates $\Gamma_{\pi\sigma}$ and $\Gamma_{\sigma\pi}$. We optimized the diffusivity ratio $\eta=D_\pi/D_\sigma$ and interband scattering parameter $g=(\Gamma_{\sigma\pi}+\Gamma_{\pi\sigma})\nabla/2\pi k_B T_{c0}$ to fit the measurements using Eq. (1) from Ref. 8 as described elsewhere.[11]

The upward curvature, characteristic of the presence of two gaps,[9,10] is apparent in these $H_{c2}(T)$ data. The inset displays the $H_{c2}(0)$ extrapolations and the fit parameters $1/D_\pi$, $1/D_\sigma$ as function of x. We observe that $H_{c2}(0)$ increases with x and has a good correlation with the fit parameter behavior. This enhancement is the result of changes in the diffusivity coefficients, as a consequence of C incorporation in the B site, affecting not only the σ band but also the π band. Changes in the interband scattering coefficient are also reflected in T_c decrease.[8]

The CNT additions produce a larger C incorporation than SiC, probably because of the higher synthesis temperature, resulting in samples with lower T_c. The dwCNT sample has the highest C content into the lattice, indicating that using this kind of inclusions is an easier way to incorporate C. This allows to reach a record H_{c2} value for this sample. Earlier MgB_2 carbon doped data from Wilke *et al.*[22,23] also indicate an initial rapid rise for lower C contents that then slows down, reaches a maximum at intermediate carbon concentrations, and decreases for larger C contents and the same behavior was reported for MgB_2 single crystals.[30] The $H_{c2}(0)$ of dwCNT is close to the maximum H_{c2} value as a function of x.[11] A decrease in $H_{c2}(0)$ was also observed for a larger x

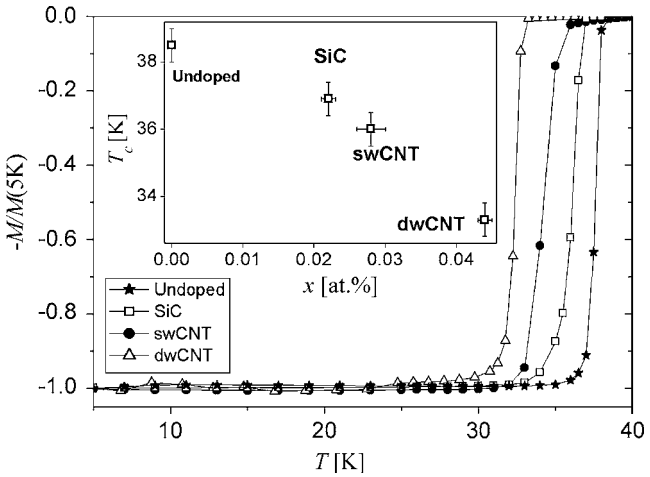

FIG. 1. Normalized zero field cooling magnetization as a function of temperature for all samples of Table I. The inset shows T_c onset vs the actual C content (x) as determined by a-axis lattice parameter.

Downloaded 04 Sep 2008 to 130.130.37.13. Redistribution subject to AIP license or copyright; see http://jap.aip.org/jap/copyright.jsp

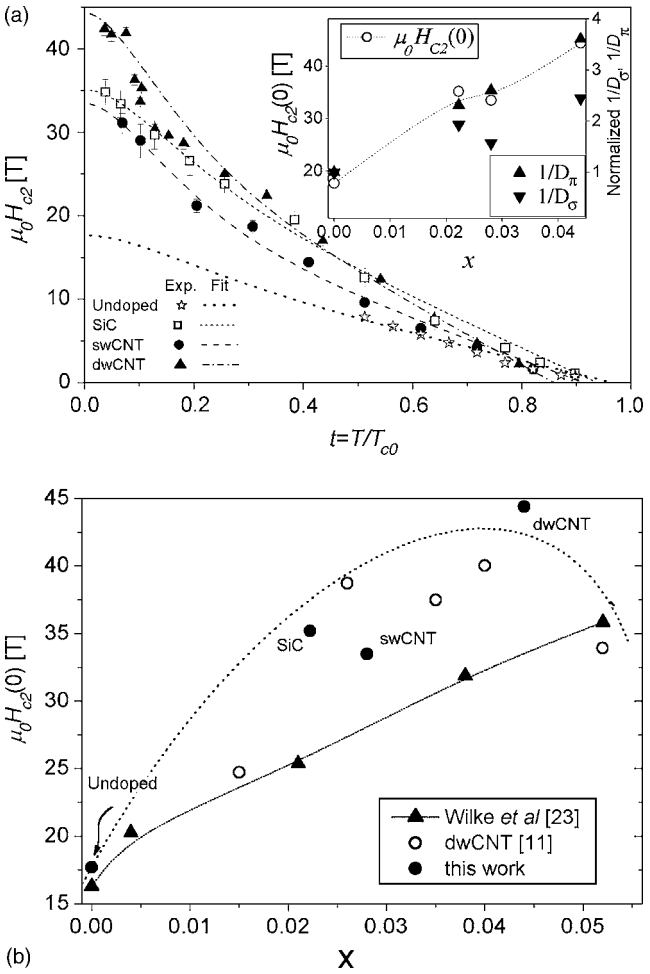

FIG. 2. Upper critical field (H_{c2}) vs $t=T/T_{c0}$ from transport experiments (symbols), where $T_{c0}=39$ K (Ref. 29) and H_{c2} was defined at the onset of the $R(H)$ curves for all samples. Dashed lines correspond to fits using Eq. (1) in Ref. 11. The inset shows the dependence of H_{c2} extrapolated to 0 K, normalized $1/D_\pi$ and $1/D_\sigma$ with x (dotted lines are guides to the eyes).

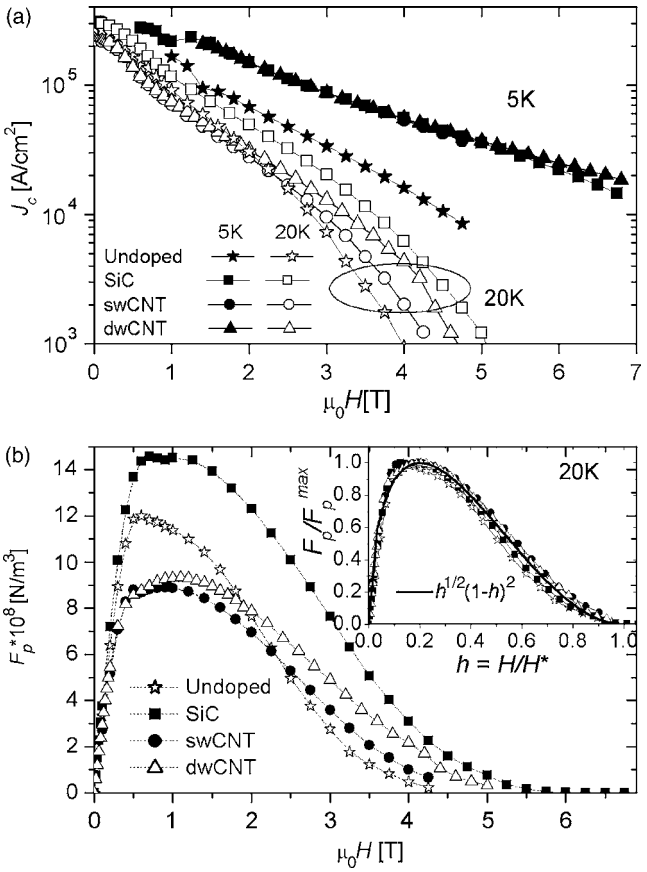

FIG. 3. (a) J_c field dependence obtained from magnetization loops for all samples described in Table I at 5 K (solid symbols) and 20 K (open symbols). (b) F_p as a function of the applied field of all four samples at 20 K. The inset shows the same normalized F_p as a function of the reduced field where the criterion for H^* is $J_c=100$ A/cm^2. The full line is the theoretical field dependence of F_p/F_p^{max} proposed for the grain boundary flux pinning.

value [see Fig. 2(b)], in agreement with very recently reported data.[28] Matsumoto *et al.*[26] reported a similar to our record $H_{c2}(0)$ value for a SiC-doped MgB_2 tape prepared by the powder-in-tube (PIT) method. These results correspond to a PIT tape sample that probably has some texturing[31–33] and the reported H_{c2} data were measured with the applied field parallel to the tape. Since we measured randomly oriented polycrystalline bulk samples, our results cannot be easily compared with those of Matsumoto *et al.*

The field dependences for J_c, calculated from magnetization using the Bean model,[34] at 5 and 20 K are illustrated in Fig. 3(a). The J_c enhancement indicates that both CNT and SiC increase the amount of pinning centers with respect to the undoped sample. This improvement comes part from C doping, and part may come from an improvement in connectivity and/or the pinning effect of the possible remaining CNTs, or the presence of other defects as a consequence of SiC addition, respectively. The variation between J_c's may be due to the different defect sizes and distribution (swCNT, dwCNT, and SiC). The dwCNT sample displays a slightly higher J_c at 5 K above 5 T while the SiC's J_c is larger than the others in the whole field range at 20 K including a J_c self-field improvement. A crude estimation of the pinning force due to small precipitates in MgB_2 indicates that the smaller the size, the higher must be the density of those defects to be effective.[1] In particular, if we consider the di-

TABLE II. Reduced temperature $t=T/T_{c0}$, residual resistivity ratio (RRR)$=\rho(295\text{ K})/\rho(40\text{ K})$, and parameters D_σ and D_π obtained by fitting $H_{c2}(T)$ curves with Eq. (1) of Ref. 11 (for complete explanation see Refs. 7 and 8).

Sample	t	D_σ	D_π	$\sim H_{c2}(0)$ (T)	RRR	$\rho(40\text{ K})$ ($\mu\Omega$ cm)
Undoped	0.987	0.56×10^{-4}	1×10^{-5}	17.7	2.2	90
SiC	0.945	0.29×10^{-4}	4.328×10^{-6}	35.2	1.74	300[a]
swCNT	0.923	0.357×10^{-4}	3.838×10^{-6}	33.5	1.41	91
dwCNT	0.854	0.229×10^{-4}	2.772×10^{-6}	44.4	1.38	<80

[a]Reference 13.

Downloaded 04 Sep 2008 to 130.130.37.13. Redistribution subject to AIP license or copyright; see http://jap.aip.org/jap/copyright.jsp

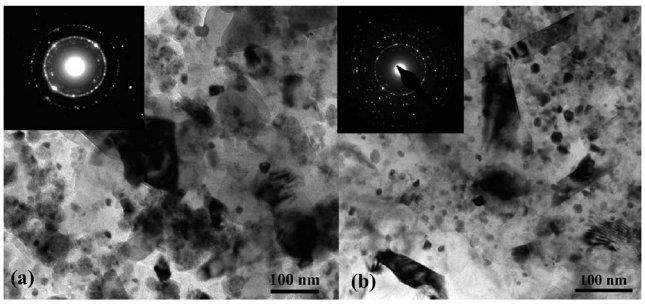

FIG. 4. Bright-field images of the (a) SiC and (b) swCNT samples showing the characteristic grain sizes and precipitates of doped MgB_2. The insets show selected area diffraction patterns indicative of polycrystalline structure in both samples, where diffraction rings from the amorphous or secondary phases appear only in the inset (a).

ameter size of swCNT ~1.1 nm, a very high density ($>10^{16}$ defects/cm^3) would be necessary to pin the vortices. Energy filtered transmission electron microscopy images of the swCNT sample showed some C-rich regions, in which C seems to be separated from the other elements (i.e., B, Mg), asserting the idea that some CNTs did not dissolve in the MgB_2 matrix. We calculated approximately the density of nanotubes considering that all C that is not incorporated into the MgB_2 lattice (i.e., the difference between nominal and x content) remains as CNT, obtaining $\sim 4\times 10^{15}$ defects/cm^3 for dwCNT and $\sim 4\times 10^{14}$ defects/cm^3 for swCNT. In the last case the amount of defects is far below the required amount, which may explain the lower J_c values in this sample at higher fields and $T=20$ K.

A rough approximation of the connectivity in these samples can be calculated using a modified Rowell analysis[35] for C-doped samples proposed by Senkowicz *et al.*[27] According to the resistivity data in Table II CNT samples have larger connectivity (>30%) than the undoped sample (~6%) while the SiC sample has the worst connectivity (<5%). Therefore, the J_c enhancement in CNT-doped samples may also come from improved connectivity.

It is clear from Fig. 3(a) that the irreversibility field H^* is largely improved for the doped samples at 20 K, especially for SiC. This enhancement can also be observed in Fig. 3(b) that displays the pinning force ($F_p=J_c^*\mu_0 H$) as a function of the applied field. A shift in the maximum F_p's and a clear enhance of F_p are observed at higher fields for all doped samples. The microstructure of all doped samples exhibits small grains, while the undoped sample presents larger grains (~1 μm).[18]. Figure 4 illustrates the microstructure of (a) SiC and (b) swCNT samples with regions of grains from 20 to 100 nm. Scanning electron microscopy observations of both CNT samples exhibited similar microstructures. The insets in Fig. 4 exhibit only MgB_2 diffraction spots for the CNT sample while diffraction rings from the amorphous or secondary phases appear for the SiC sample. In the normalized plot [see inset of Fig. 3(b)] all curves are very close to each other. A comparison of the F_p field dependence of our samples with the theoretical dependence proposed for the grain boundary flux pinning [$F_p/F_p^{\max}\propto h^{1/2}(1-h)^2$, where $h=H/H^*$] (Ref. 36) is not clear enough to understand the influence of the different additions in the pinning properties). The normalized F_p's are slightly higher than the expected for grain boundary flux pinning, which indicates that the CNT additions resulted in an additional pinning. This extra pinning effect and the better grain connectivity are not so effective due to a T_c decrease (see Table I). In contrast, SiC sample presents a very low connectivity, so the improved in-field J_c is due to a stronger pinning. Several potential pinning centers were introduced by SiC doping shown secondary phases in Fig. 4, including $MgSi_2$, BC, BO_x, $SiBO_x$, and unreacted SiC as identified by electron-energy-loss spectroscopy and x-ray diffraction, which are all at a scale below 10 nm, and provide effective pinning at all the temperatures up to T_c.[13]

The improvement in J_c is not linearly related to x, and it is not clear whether C incorporation, or the remaining intra- or intergrain defects, is the predominant effect. It is worthy to note that SiC may produce the best pinning effect owing to the following factors: C substitution induced embedded defects within grains and a strong grain boundary pinning due to low processing temperature.[12,13] Nanoscale SiC can react with Mg at temperatures as low as 600 °C at which MgB_2 formation takes place. The free C released from the reaction can be easily incorporated into the lattice while the nanoscale impurities such as Mg_2Si are included in the grains as nanoinclusions.[13] Low temperature processing produces small grains and unreacted impurities with a high density of nanoscale defects, which act as effective pinning centers. In contrast, C substitution for B in CNT-doped samples was only achieved at higher temperatures (900 °C). Thus, flux pinning in CNT-doped samples is not as strong as in SiC-doped samples at high temperatures apparently due to a decrease in T_c and a low density of defects.

IV. SUMMARY

In summary, we found that additions of SiC or CNT produce simultaneous enhancement of J_c and H_{c2}, but there is a clear difference in the origin of flux pinning effects in both cases. Nano-SiC is more effective to improve the flux pinning at high temperatures (i.e., 20 K), and this improvement cannot be solely attributed to the C incorporation to the lattice but to the presence of high density of defects including grain boundaries and also other nanoprecipitates. On the contrary, CNTs produce a better C incorporation that is more effective to enhance H_{c2}, reaching a record $H_{c2}(0)$ value for bulk dwCNT MgB_2, but the enhancement of J_c, which is very good at 5 K, is not as good as SiC at 20 K. Finally, the measured $H_{c2}(T)$ in all samples are successfully described using a theoretical model for a two-gap superconductor in the dirty limit, and corroborates that the C incorporation to the lattice is correlated with the π-band scattering.

ACKNOWLEDGMENTS

This work was supported at Centro Atómico Bariloche by CONICET, Fundación Antorchas, and SECyT-PICT; at Los Alamos National Laboratory by the Office of Electricity Delivery and Energy Reliability, US Department of Energy; at Wollongong by Australian Research Council and Hyper

Downloaded 04 Sep 2008 to 130.130.37.13. Redistribution subject to AIP license or copyright; see http://jap.aip.org/jap/copyright.jsp

Tech Research Inc.; and at the NHMFL by the US National Science Foundation, the State of Florida, and the US Department of Energy.

[1]X. Z. Liao, A. Serquis, Y. T. Zhu, J. Y. Huang, L. Civale, D. E. Peterson, H. F. Xu, and F. M. Mueller, J. Appl. Phys. **93**, 6208 (2003).
[2]S. H. Zhou, A. V. Pan, M. J. Qin, H. K. Liu, and S. X. Dou, Physica C **387**, 321 (2003).
[3]A. Berenov, A. Serquis, X. Z. Liao, Y. T. Zhu, D. E. Peterson, Y. Bugoslavsky, K. A. Yates, M. G. Blamire, L. F. Cohen, and J. L. MacManus-Driscoll, Supercond. Sci. Technol. **17**, 1093 (2004).
[4]S. K. Chen, M. Wei, and J. L. MacManus-Driscoll, Appl. Phys. Lett. **88**, 192512 (2006).
[5]S. X. Dou, J. Horvat, S. Soltanian, X. L. Wang, M. J. Qin, S. H. Zhou, H. K. Liu, and P. G. Munroe, IEEE Trans. Appl. Supercond. **13**, 3199 (2003).
[6]S. X. Dou, W. K. Yeoh, J. Horvat, and M. Ionescu, Appl. Phys. Lett. **83**, 4996 (2003).
[7]A. Gurevich, Phys. Rev. B **67**, 184515 (2003).
[8]V. Braccini, A. Gurevich, J. E. Giencke, M. C. Jewell, C. B. Eom, D. C. Larbalestier, A. Pogrebnyakov, Y. Cui, B. T. Liu, Y. F. Hu, J. M. Redwing, Q. Li, X. X. Xi, R. K. Singh, R. Gandikota, J. Kim, B. Wilkens, N. Newman, J. Rowell, B. Moeckly, V. Ferrando, C. Tarantini, D. Marré, M. Putti, C. Ferdeghini, R. Vaglio, and E. Haanappel, Phys. Rev. B **71**, 012504 (2005).
[9]A. A. Golubov, J. Kortus, O. V. Dolgov, O. Jepsen, Y. Kong, O. K. Andersen, B. J. Gibson, K. Ahn, and R. K. Kremer, J. Phys.: Condens. Matter **14**, 1353 (2002).
[10]A. Gurevich, S. Patnaik, V. Braccini, K. H. Kim, C. Mielke, X. Song, L. D. Cooley, S. D. Bu, D. M. Kim, J. H. Choi, L. J. Belenky, J. Giencke, M. K. Lee, W. Tian, X. Q. Pan, A. Siri, E. E. Hellstrom, C. B. Eom, and D. C. Larbalestier, Supercond. Sci. Technol. **17**, 278 (2004).
[11]A. Serquis, G. Serrano, S. Moreno, L. Civale, B. Maiorov, F. Balakirev, and M. Jaime, Supercond. Sci. Technol. **20**, L12 (2007).
[12]S. X. Dou, S. Soltanian, J. Horvat, X. L. Wang, P. Munroe, S. H. Zhou, M. Ionescu, H. K. Liu, and M. Tomsic, Appl. Phys. Lett. **81**, 3419 (2002).
[13]S. X. Dou, V. Braccini, S. Soltanian, R. Klie, Y. Zhu, S. Li, X. L. Wang, and D. Larbalestier, J. Appl. Phys. **96**, 7549 (2004).
[14]W. K. Yeoh, J. Horvat, S. X. Dou, and V. Keast, Supercond. Sci. Technol. **17**, S572 (2004).
[15]W. K. Yeoh, J. Horvat, S. X. Dou, and P. Munroe, IEEE Trans. Appl. Supercond. **15**, 3284 (2005).
[16]W. K. Yeoh, J. H. Kim, J. Horvat, S. X. Dou, and P. Munroe, Supercond. Sci. Technol. **19**, L5 (2006).
[17]A. Serquis, Y. T. Zhu, E. J. Peterson, J. Y. Coulter, D. E. Peterson, and F. M. Mueller, Appl. Phys. Lett. **79**, 4399 (2001).
[18]A. Serquis, X. Z. Liao, Y. T. Zhu, J. Y. Coulter, J. Y. Huang, J. O. Willis, D. E. Peterson, F. M. Mueller, N. O. Moreno, J. D. Thompson, V. F. Nesterenko, and S. S. Indrakanti, J. Appl. Phys. **92**, 351 (2002).
[19]S. X. Dou, W. K. Yeoh, O. Shcherbakova, J. H. Kim, J. Horvat, A. V. Pan, Y. Li, W. X. Li, Z. M. Ren, and P. Munroe, Appl. Phys. Lett. **89**, 202504 (2006).
[20]A. Yamamoto, J. Shimoyama, S. Ueda, Y. Katsura, I. Iwayama, S. Horii, and K. Kishio, Physica C **445–448**, 806 (2006).
[21]X. S. Huang, W. Mickelson, B. C. Regan, and A. Zettl, Solid State Commun. **136**, 278 (2005).
[22]R. H. T. Wilke, S. L. Bud'ko, P. C. Candfield, D. K. Finnemore, R. J. Suplinskas, and S. T. Hannahs, Phys. Rev. Lett. **92**, 217003 (2004).
[23]R. H. T. Wilke, S. L. Bud'ko, P. C. Canfield, D. K. Finnemore, R. J. Suplinskas, and S. T. Hannahs, Physica C **424**, 1 (2005).
[24]B. J. Senkowicz, J. E. Giencke, S. Patnaik, C. B. Eom, E. E. Hellstrom, and D. C. Larbalestier, Appl. Phys. Lett. **86**, 202502 (2005).
[25]S. M. Kazakov, R. Puzniak, K. Rogacki, A. V. Mironov, N. D. Zhigadlo, J. Jun, Ch. Soltmann, B. Batlogg, and J. Karpinski, Phys. Rev. B **71**, 024533 (2005).
[26]A. Matsumoto, H. Kumakura, H. Kitaguchi, B. J. Senkowicz, M. C. Jewell, E. E. Hellstrom, Y. Zhu, P. M. Voyles, and D. C. Larbalestier, Appl. Phys. Lett. **89**, 132508 (2006).
[27]M. Avdeev, J. D. Jorgensen, R. A. Ribeiro, S. L. Bud'ko, and P. C. Canfield, Physica C **387**, 301 (2003).
[28]B. J. Senkowicz, A. Polyanskii, R. J. Mungall, Y. Zhu, J. E. Giencke, P. M. Voyles, C. B. Eom, E. E. Hellstrom, and D. C. Larbalestier, Supercond. Sci. Technol. **20**, 650 (2007).
[29]In Refs. 7 and 11 is defined $T_{c0}=T_c(g=0)$ with g the interband scattering parameter. This value corresponds to the clean limit MgB_2 sample.
[30]T. Masui, S. Lee, A. Yamamoto, H. Uchiyama, and S. Tajima, Physica C **412–414**, 303 (2004).
[31]P. Kováč, T. Melišek, and I. Hušek, Supercond. Sci. Technol. **18**, L45 (2005).
[32]R. Flükiger, P. Lezza, C. Beneduce, N. Musolino, and H. L. Suo, Supercond. Sci. Technol. **16**, 264 (2003).
[33]W. Goldacker, S. I. Schlachter, H. Reiner, S. Zimmer, B. Obst, H. Kiesel, and A. Nyilas, in *Studies of High Temperature Superconductors*, edited by A. Narlikar (Nova Science, New York, 2002), Vol. 45.
[34]C. P. Bean, Phys. Rev. Lett. **8**, 250 (1962).
[35]J. M. Rowell, Supercond. Sci. Technol. **16**, R17 (2003).
[36]D. Hughes, Philos. Mag. B **55**, 459 (1987).

Downloaded 04 Sep 2008 to 130.130.37.13. Redistribution subject to AIP license or copyright; see http://jap.aip.org/jap/copyright.jsp